Alternating-Gradient Focusing and Related Properties of Conventional Convergent Lens Focusing

By S. E. MILLER

(Manuscript received June 8, 1964)

A series of lenses whose focusing properties are alternately convergent and divergent (alternating-gradient focusing) is of potential interest in the guidance of light waves, and has previously been used to focus electron beams and high-energy particle streams. New information is provided herein on such focusing for the case of equal focal length f (but alternating-gradient) lenses equally spaced a distance L.

The alternating-gradient system formed by adding diverging lenses between the lenses of an all-converging sequence of lenses is found to have the same stability condition as the original system for $0 < L/f < 2$. A physical argument leads to the conclusion that weaker divergent lenses would also leave the stability criterion unchanged.

The focusing effect of the alternating-gradient system is surprisingly close to that of an all-converging lens system. After the focal length of each has been adjusted to an optimum value, the ray departure from the system axis is only 1.67 times as great for the alternating-gradient system as for an all-convergent lens system with the same spacing of convergent lenses.

For weak lenses (i.e. $2f/L \gg 1$) the output ray departure due to input ray displacement is independent of both the focal length and spacing of the lenses, and is independent of lens spacing but proportional to focal length for input ray slope.

Both the alternating-gradient system and all-convergent lens focusing arrangements exhibit discontinuities in the maximum ray displacement versus focal strength relation.

Viewed over-all, alternating-gradient focusing for light guidance does a surprisingly efficient job and may be advantageous over all-convergent lens systems if the alternating-gradient arrangement has structural or economic advantages.

I. INTRODUCTION

In research on guidance of light waves for communication we are considering use of a sequence of lenses of alternately convergent and divergent types. For example, a guidance system using tubular thermal gas lenses might employ continuous flow of gas through a tube whose walls are alternately warmer and cooler than the gas within. Thus, the mechanism used to cause the focusing may have the alternating character, and the question comes to the fore — how well can one focus with such a structure as compared to the use of a sequence of all-convergent lenses?

Alternating-gradient focusing has previously been used on electron beams[1] and on particle accelerators.[2] The present study discovered an error in the previous determination of stability conditions and revealed some little known but interesting properties of alternating-gradient focusing. A comparison is made with conventional focusing using all-convergent lenses.

II. ANALYSIS OF ALTERNATING-GRADIENT SYSTEMS

One might wonder whether a series of equal-focal-length and alternately converging and diverging lenses would give any net focusing at all, since the average dielectric constant along all paths parallel to the axis would be the same. It is well known, however, that a divergent lens followed by a convergent lens of equal focal length, spaced a finite distance less than the focal length, gives a net *converging* lens, and the same is true if the order of the lenses is reversed. Thus, a net focusing is to be expected for an infinite series of such lens pairs.[1]

We consider a sequence of alternating convergent and divergent lenses equally spaced a distance L and of equal focal lengths, f. We follow the method of analysis used by Pierce.[1] There are two cases to cover, one in which the first lens of the array is a divergent lens (obtained by starting at $n = 0$ in Fig. 1) and the other in which the first lens of the array is a convergent lens (obtained by starting at $N = 0$ in Fig. 4, below).

With reference to Fig. 2, and taking the input ray at plane a to have a slope r_a' and a displacement r_a from the longitudinal axis, the output ray from the lens at plane b will be

$$r_b = r_a + Lr_a' \tag{1}$$

$$r_b' = r_a' + (1/f)r_b\,. \tag{2}$$

At plane c this ray will be described by

$$r_c = r_b + Lr_b' \tag{3}$$

$$r_c' = r_b'. \tag{4}$$

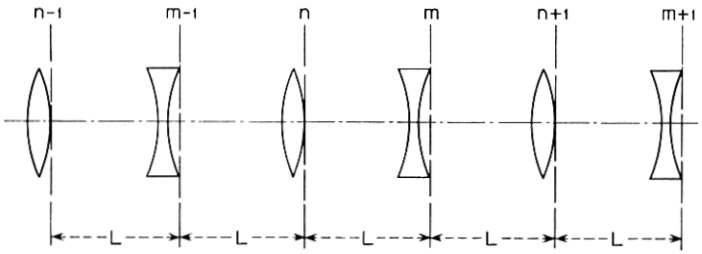

Fig. 1 — Sequence of lenses — first case.

Eliminating r_b and r_b' from (3) and (4) gives

$$r_c = \left(1 + \frac{L}{f}\right) r_a + L\left(2 + \frac{L}{f}\right) r_a' \tag{5}$$

$$r_c' = \left(1 + \frac{L}{f}\right) r_a' + \frac{r_a}{f}. \tag{6}$$

Hence, with reference to Fig. 1, we can write

$$r_{n+1} = \left(1 + \frac{L}{f}\right) r_n + L\left(2 + \frac{L}{f}\right) r_n' \tag{7}$$

$$r_{n+1}' = \left(1 + \frac{L}{f}\right) r_n' + \frac{r_n}{f} - \frac{r_{n+1}}{f}. \tag{8}$$

These two equations lead to

$$r_{n+2} - \left[2 - \left(\frac{L}{f}\right)^2\right] r_{n+1} + r_n = 0. \tag{9}$$

The solution to (9) is

$$r_n = A \cos n\theta + B \sin n\theta \tag{10}$$

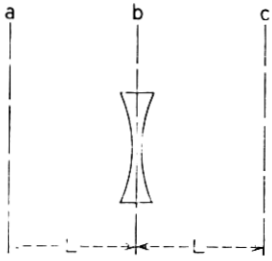

Fig. 2 — Lens subsection for Fig. 1.

where

$$\theta = \cos^{-1}\left[1 - \frac{1}{2}\left(\frac{L}{f}\right)^2\right] \tag{11}$$

and where A and B are constants to be determined.

Equation (11) differs from the corresponding equation on page 200 of Ref. (1), which is believed to be in error. The correct condition for stability, from (11), is

$$0 < \tfrac{1}{2}(L/f)^2 < 2 \tag{12}$$

or

$$0 < L/f < 2.$$

We put in the boundary conditions, at $n = 0$

$$r_n' = r_0' \tag{13}$$

$$r_n = r_0 . \tag{14}$$

We make use of a general theorem* stating the orthogonality of the effects of r_0 and r_0' and seek a solution with those quantities as factors. This leads to the following form for r_n, using (10), (7), (13) and (14):

$$r_n = r_0 k_1 \cos(n\theta - \varphi_1) + r_0' L\, k_2 \sin n\theta \tag{15}$$

where

$$k_1 = \left[\frac{2}{1 - (L/2f)}\right]^{\frac{1}{2}} \tag{16}$$

$$\varphi_1 = |\cos^{-1} k_1^{-1}| \tag{17}$$

$$k_2 = \frac{[(2f/L) + 1]}{[1 - \frac{1}{4}(L/f)^2]^{\frac{1}{2}}} = \frac{[2 + (L/f)]}{\sin\theta} . \tag{18}$$

The general form of k_1 and k_2 versus L/f is shown in Fig. 3. Further discussion will be postponed to a later point in this paper.

We are also interested in the displacement r_m at the output of the mth diverging lens (Fig. 1). Using the relation

$$r_m = r_n + Lr_n' \tag{19}$$

and using (7) for r_n', (15) for r_n with appropriate trigonometric relations, it can be shown that

$$r_m = r_0 k_3 \cos(m\theta - \varphi_3) + r_0' L\, k_4 \cos(m\theta - \varphi_4) \tag{20}$$

* See Appendix B.

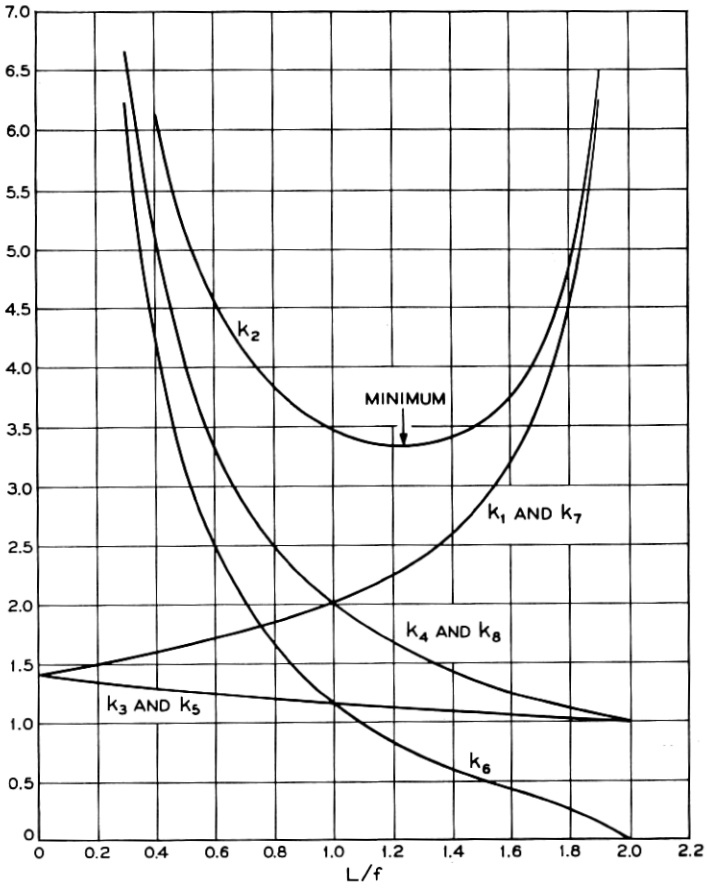

Fig. 3 — Coefficients relating input ray slope and displacement to ray displacement at the nth, mth, Nth, and Mth lenses of the alternating-gradient lens systems of Figs. 1 and 4.

where

$$k_3 = \left[\frac{2}{1 + (L/2f)}\right]^{\frac{1}{2}} \tag{21}$$

$$\varphi_3 = |\cos^{-1} k_3^{-1}| \tag{22}$$

$$k_4 = 2f/L \tag{23}$$

$$\varphi_4 = |\cos^{-1} k_4^{-1}| \tag{24}$$

and θ is again defined by (11). Plots of k_3 and k_4 are given in Fig. 3.

Equations (15) and (20) give the ray displacements at any lens in the system when the input is at a plane adjacent to a converging lens (i.e. at $n = 0$, Fig. 1). Before discussing interesting features of such ray propagation we will give the corresponding solutions for the case where the input is adjacent to a diverging lens (i.e. at $N = 0$, Fig. 4).

With reference to Figs. 4 and 5, and following a derivation similar to that carried out in connection with equations (1) to (9), it is found that

$$r_{N+2} - [2 - (L/f)^2]\, r_{N+1} + r_N = 0. \tag{25}$$

Note that (25) is identical to (9) and with the change of n into N the solution for (25) is again (10) and (11). When the initial conditions are put in, at $N = 0$, $r_N = r_0$ and $r_N' = r_0'$, we get

$$r_N = r_0 k_r \cos(N\theta + \varphi_5) + r_0' L k_6 \sin N\theta \tag{26}$$

where

$$k_5 = \frac{(L/f)[2 - (L/f)]^{\frac{1}{2}}}{\sin\theta} = \left[\frac{2}{1 + (L/2f)}\right]^{\frac{1}{2}} \tag{27}$$

$$\varphi_5 = |\cos^{-1} k_5^{-1}| \tag{28}$$

$$k_6 = \frac{[(2f/L) - 1]}{[1 - \frac{1}{4}(L/f)^2]^{\frac{1}{2}}} = \frac{[2 - (L/f)]}{\sin\theta}. \tag{29}$$

Note that k_5 is identical to k_3 in (21).

For r_M we find

$$r_M = r_0 k_7 \cos(M\theta + \varphi_7) + r_0' L k_8 \sin(M\theta - \varphi_8) \tag{30}$$

where

$$k_7 = \left[\frac{2}{1 - (L/2f)}\right]^{\frac{1}{2}} \tag{31}$$

$$\varphi_7 = |\cos^{-1} k_7^{-1}| \tag{32}$$

$$k_8 = 2f/L \tag{33}$$

$$\varphi_8 = |\cos^{-1} k_8^{-1}|. \tag{34}$$

Note that k_8 and φ_8 are identical to k_4 and φ_4, and that k_7 is identical to k_1. Plots of k_5, k_6, k_7, k_8 are given in Fig. 3.

III. RELATIONS FOR A SEQUENCE OF CONVERGING LENSES

For comparison purposes we will want to refer to the case of a sequence of identical convergent lenses equally spaced. The analysis is similar to that above for the alternating gradient lenses. The results are

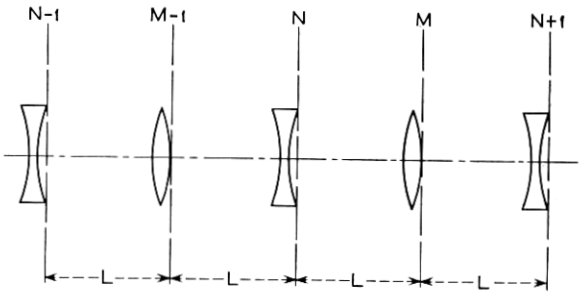

Fig. 4 — Sequence of lenses — second case.

as follows. Let the lens spacing be s, and the focal length be f. Then the displacement r_p at the pth lens is

$$r_p = r_0 k_9 \cos(p\delta - \varphi_9) + r_0' s\, k_{10} \sin p\delta \tag{35}$$

where

$$k_9 = \left[\frac{4f/s}{(4f/s) - 1}\right]^{\frac{1}{2}} \tag{36}$$

$$\varphi_9 = |\cos^{-1} k_9^{-1}| \tag{37}$$

$$k_{10} = \frac{(f/s)^{\frac{1}{2}}}{[1 - (s/4f)]^{\frac{1}{2}}} = \frac{1}{\sin\delta} \tag{38}$$

$$\delta = \cos^{-1}[1 - (s/2f)] \tag{39}$$

$$s/f = 2(1 - \cos\delta). \tag{40}$$

The system is stable in the sense that an input displacement r_0 or slope r_0' will remain bounded as p is increased if

$$0 < s/f < 4. \tag{41}$$

Fig. 6 shows the values of k_9 and k_{10} for comparison to Fig. 3.

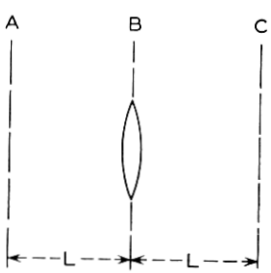

Fig. 5 — Lens subsection for Fig. 4.

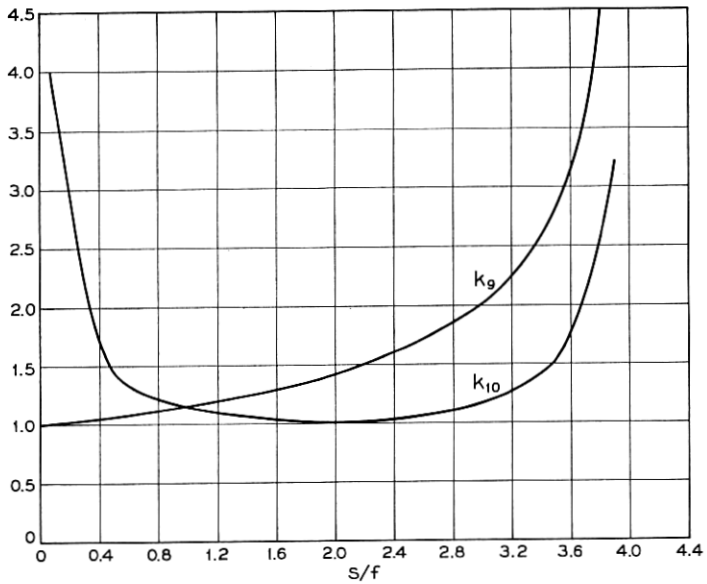

Fig. 6 — Coefficients relating ray slope and displacement to ray displacement at the pth lens of an all-convergent lens system; f = focal length, s = lens spacing.

IV. STABILITY COMPARISON

Since the converging lenses in Fig. 1 or Fig. 4 are spaced a distance $2L$, a comparison of (41) and (12) shows that the alternating-gradient system formed by adding a divergent lens halfway between the convergent lenses of an all-convergent lens system has the same stability condition as the original system. At a later point it will be shown that this is reasonable physically.

V. THE WEAK LENS CASE

When the lenses are weak, i.e., when $2f/L \gg 1$, the general expressions may be simplified to show some remarkable properties of alternating-gradient focusing. When the first lens is a diverging one, (15) and (20) yield

$$r_m = r_n = r_0 \sqrt{2} \cos [n\theta - (\pi/4)] + r_0' 2f \sin n\theta \qquad (42)$$

and when the first lens is a converging one, (26) and (30) yield

$$r_N = r_M = r_0 \sqrt{2} \cos [N\theta + (\pi/4)] + r_0' 2f \sin N\theta. \qquad (43)$$

These expressions show that for an input ray displacement without

slope the maximum displacement of the transmitted ray (as n or N varies) is $\sqrt{2}$ times the input ray displacement, independent of both focal length and lens spacing! Also, for an input ray of zero displacement but finite slope r_0', the maximum displacement of the transmitted ray is $2fr_0'$, independent of lens spacing L. The angle θ is dependent on f and L and goes to zero as $f \to \infty$.

In an all-convergent lens system the similar condition $4f/s \gg 1$ leads to [from (35)]

$$r_p = r_0 \cos p\delta + r_0' \sqrt{fs} \sin p\delta. \tag{44}$$

In comparing the alternating-gradient system to the all-convergent lens system for weak lenses, we see that for an input ray with zero slope r_0' but finite displacement, r_0, the maximum output displacement for the alternating-gradient system is $\sqrt{2}$ times that of the all-convergent lens system. For input ray displacement $r_0 = 0$ but finite r_0', we see that the maximum output displacement for the alternating-gradient system is larger than for the all-converging lens system by the factor [see (42) and (44)]:

$$\frac{2fr_0'}{(fs)^{\frac{1}{2}}r_0'} = (4f/s)^{\frac{1}{2}}. \tag{45}$$

Our assumption of weak lenses made $4f/s \gg 1$, so (45) is a factor of two or more.

In this weak lens case both θ and δ are small angles, and from (11) and (39)

$$\theta \cong L/f \tag{46}$$

$$\delta \cong (s/f)^{\frac{1}{2}}. \tag{47}$$

Using the case of $s = 2L$, which is the alternating-gradient system formed by adding a diverging lens between the lenses of an all-convergent lens system

$$\theta/\delta = (s/4f)^{\frac{1}{2}}. \tag{48}$$

Since $4f/s \gg 1$ by our weak lens definition, θ/δ is less than unity and the period of the alternating-gradient system encompasses a great many more convergent lenses than does the all-convergent lens system with the same spacing of convergent lenses. This is as would be expected.

VI. OPTIMUM FOCAL LENGTHS

We now inquire as to whether there is a best value for the lens strength in order to minimize output ray displacement. On the assumption that

the sine and cosine terms of (15), (20), (26), (30) and (35) go through unity for some number of lenses, the question is whether or not the coefficients k_1, $k_2 \cdots k_{10}$ have any minima.

For the all-convergent lens system Fig. 6 illustrates that k_9 has no useful minimum but that k_{10}, relating input ray slope to output ray displacement as in (35), does have a minimum. By setting

$$\frac{d}{df}(k_{10}) = 0 \tag{49}$$

we find

$$\left.\frac{s}{f}\right|_{\text{opt}} = 2 \tag{50}$$

at which condition $k_{10} = 1.0$. We note that the displacement r_p due to r_0' is $r_0' s k_{10} \sin p\delta$, so we have a minimum in this displacement when k_{10} is a minimum provided $\sin p\delta$ goes through unity for some number of lenses p. This is the most typical case, but there are notable exceptions. Suppose, for example, that δ of (39) is $\pi/3$, corresponding to $s/f = 1$; then $p\delta = \pi/3, 2\pi/3, \pi, 4\pi/3$, etc., as illustrated in Fig. 7, and $|\sin p\delta|$ never exceeds $\sin \delta$. Hence the maximum value of $r_0' s\, k_{10} \sin p\delta$ is $r_0' s$ for $s/f = 1$. It is shown in Appendix A that there is an infinite series of such discrete values, but the largest departure of the maximum value of $r_0' s k_{10} \sin p\delta$ from k_{10} is 15 per cent, occurring at s/f values of 1 and 3, as illustrated in Fig. 14 (see Appendix A).

Turning now to the alternating-gradient system, the only coefficient having a useful minimum is k_2 of (15), relating input ray slope to ray displacement at the converging lenses of Fig. 1. We find the minimum in k_2 by setting

$$\frac{d}{df}(k_2) = 0 \tag{51}$$

which leads to the equation

$$(L/f)^3 + 4(L/f)^2 - 8 = 0. \tag{52}$$

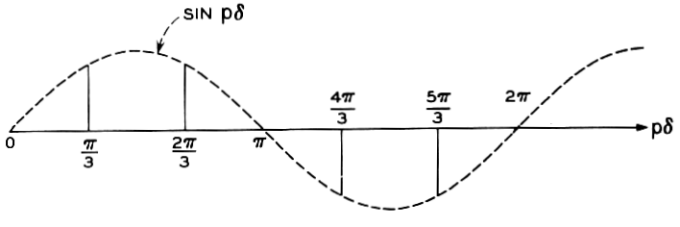

Fig. 7 — Diagram of $\sin p\delta$, $p = 1,2,3 \cdots$, when $\delta = \pi/3$.

The appropriate root of this equation is

$$\left.\frac{L}{f}\right|_{\text{opt}} = 1.237 \tag{53}$$

at which we calculate $\theta = 76.4°$, and $k_2 = 3.33$. Fig. 3 shows this minimum is sharper than the corresponding one for k_{10} of the all-converging lens system, Fig. 6. We note that $k_2 \sin n\theta$ of (15) contains the $\sin n\theta/\sin \theta$ factor, so once again (as described in Appendix A) for $\theta = \pi/3$ and other values, the maximum value of $k_2 \sin n\theta$ will be somewhat less than the value of k_2.

It is important to compare the optimized focusing effect of the alternating-gradient system to that for the all-convergent lens system. We make the comparison on the alternating-gradient system formed by adding a divergent lens of equal focal length in between the lenses of an all-convergent lens system; then we have $s = 2L$. The optimized maximum displacement due to input ray slope is

$$r_0' s = 2 r_0' L$$

for the convergent lens system, and is

$$3.33\, r_0' L$$

for the alternating-gradient system. It is remarkable that the focusing effect of the alternating-gradient system is so nearly the same as that of the all-convergent lens system. In practice it may be advantageous to get the focusing action in a manner that inherently reverses itself periodically. This analysis shows that such structures are nearly as effective as those wherein the focusing effect is always convergent.

Fig. 3 shows that the focal length which is optimum with respect to the input ray slope (k_2) is also an acceptable region with respect to input ray displacement (k_1 and k_3).

VII. RAY PATHS

One can get a useful physical feel for the wave propagation by tracing the rays in a few of the important cases.

For the all-convergent lens system optimized according to (50), Fig. 8 shows the ray paths for a zero-slope finite-displacement input ray and for a zero-displacement finite-slope input ray.* Here $\delta = 90°$ [see (35)] and a period is completed in 4 lenses. As proved in Appendix B, the

* Note that $k_9 = \sqrt{2}$, with $s = 2f$ in (36), but $k_9 \cos(p\delta - \varphi_9)$ is always ± 1 for any p. (The angle $\varphi_9 = 45°$.) This is an example of the caution that must be exercised in regarding the k's as maximum values of the various terms in r_n, r_m, r_p, etc.

response to an arbitrary input ray can be obtained by a linear superposition of the responses shown in Fig. 8.

For the alternating-gradient system the optimum according to (53) corresponds to an angle θ in (15), (20), (26) and (30) of 76.4°, which makes the ray path periodic only at a very large number of lenses. However, a very useful feel can be obtained from the ray paths for $\theta = 90°$, corresponding to $L = \sqrt{2}f$ and giving a value of k_2 only slightly larger than the minimum value (3.414 compared to 3.33). These ray plots are shown in Figs. 9 and 10 for the two types of input rays at the two possible points in the alternating-gradient system. We note that input ray displacement causes the same maximum displacement in the response regardless of where it occurs. Input ray slope is much more serious when

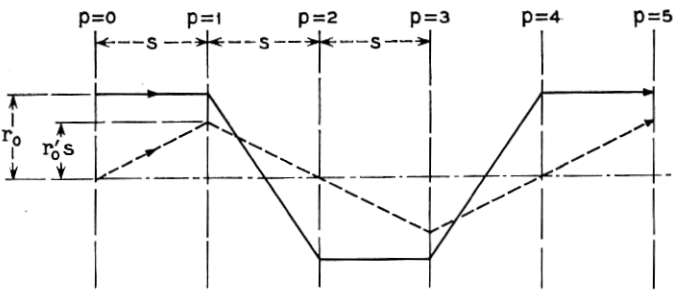

Fig. 8 — Ray paths in the confocal all-convergent lens system, $s = 2f$.

it occurs in front of a diverging lens than when it occurs in front of a converging lens. Again, the response to arbitrary input rays can be obtained by adding the plotted responses.

One can gain a little feel for the stability comparison made previously by looking at Figs. 11 and 12. Even though the r_0 term and the r_0' term of (35) for the all-convergent lens system go to infinity individually when $s = 4f$, a suitable combination of input ray slope and displacement remains bounded and this is illustrated in Fig. 11.* Any reduction in focal length f causes instability, and any increase in f leaves the system completely stable. It is clear that adding a lens of any kind at the midpoint between lenses in Fig. 11 will not alter the propagation of that ray. In Fig. 12 we see that adding a divergent lens in between the converging

* One can obtain these values of r_p from (35) by a suitable limiting process. It is helpful to start with the alternative form of (35):

$$r_p = r_0 \left\{ \cos p\delta + \frac{1}{[(4f/s) - 1]^{\frac{1}{2}}} \sin p\delta \right\} + r_0' s\, k_{10} \sin p\delta.$$

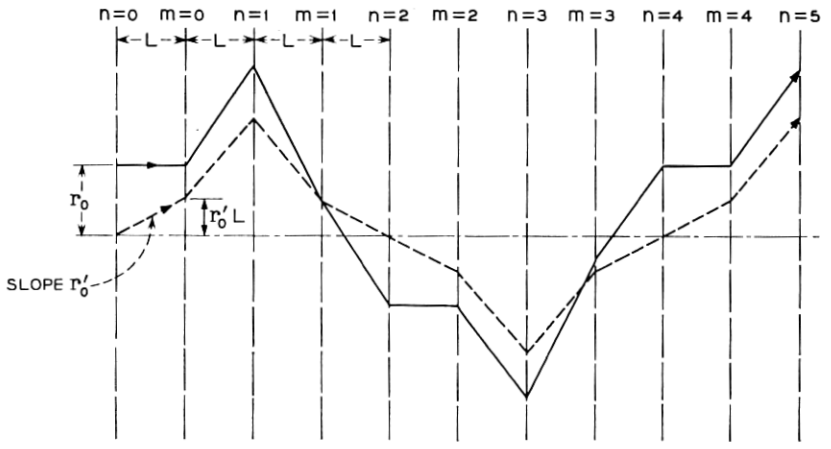

Fig. 9 — Ray paths for system of Fig. 1, $L = \sqrt{2}f$.

lenses will cause reductions in the focal length of the $p = 1$ converging lens to make the ray sent on to the $p = 2$ lens diverge even more; for increases in the focal length of the $p = 1$ lens, the divergent lens reduces the angle of the ray sent on to the $p = 2$ lens. Hence, it is plausible that the addition of the divergent lens between the convergent lenses does not alter the stability requirement on the focal lengths.

Given the mathematically-derived condition that divergent lenses of

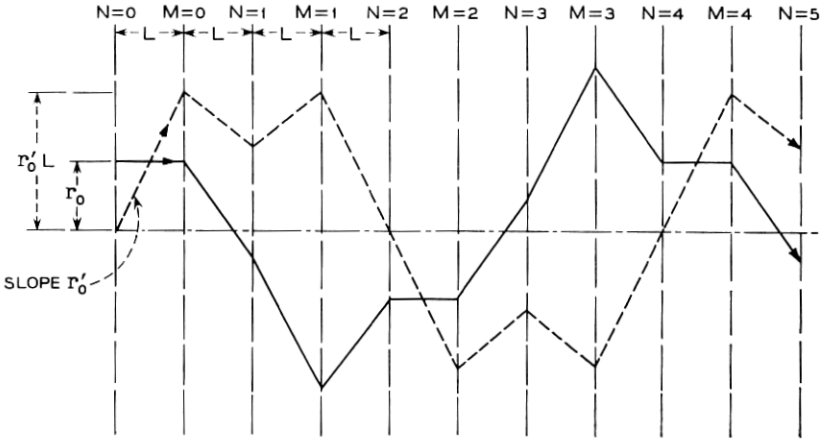

Fig. 10 — Ray paths for system of Fig. 3, $L = \sqrt{2}f$.

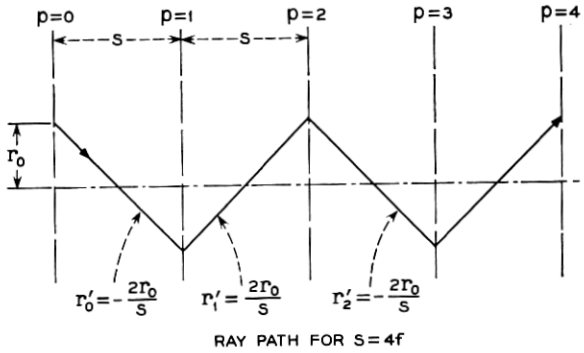

Fig. 11 — Ray path for $s = 4f$ in all-convergent lens system.

focal length f added to a chain of convergent lenses of focal length f do not change the stability criterion as described above, the physical argument just outlined leads to the conclusion that weaker divergent lenses would also leave the stability criterion unchanged.*

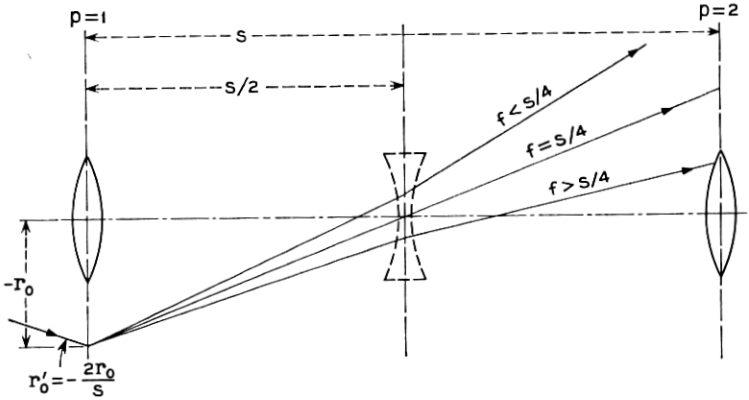

Fig. 12 — Ray path for f near $s/4$ to illustrate effect of divergent lens.

VIII. CONCLUSION

Alternating-gradient focusing is surprisingly close to an all-convergent lens system in focusing ability, and may be preferred if practical matters such as structural features or cost favor the alternating-gradient system.

* When reading this manuscript, Mr. J. P. Gordon commented that this conclusion is in agreement with the work of Boyd and Kogelnik[3] which can be shown to yield the relation $f_2 > f_1 - L/2$ for the required focal length f_2 of the diverging lens in terms of the focal length f_1 of the converging lens and the spacing L.

APPENDIX A

We examine here the maximum value that the term $r_0's$ $k_{10} \sin p\delta$ of (35) can take as a function of lens number p when our objective is to minimize the term through appropriate choice of focal length. In the body of the article it has been shown that k_{10} has a minimum at $s = 2f$. This corresponds to a value of $\delta = \pi/2$ from (39) and it is evident that $\sin p\delta = \sin p\,\pi/2$ is either zero or unity for all integral values of p.

In the more general case we want to know the value of

$$k_{10} \sin p\delta = \sin p\delta/\sin \delta. \tag{54}$$

When it is recognized that p may take on all integral values greater than zero it follows that the maximum value of $[(\sin p\delta)/\sin \delta]$ as p varies can never be less than unity for any fixed δ.

It is possible for $[(\sin p\delta)/\sin \delta]$ to have a maximum value which is smaller than $k_{10} = 1/\sin \delta$. That is to say, $\sin p\delta$ does not necessarily go through unity even though p ranges from 0 to ∞ in integral steps.

Referring to Fig. 13, the maximum value of $\sin p\delta$ will be less than unity if

$$\delta(q + \tfrac{1}{2}) = \pi/2 \tag{55}$$

or

$$\delta = \pi/(2q + 1) \tag{56}$$

where $q = 1, 2, 3, \cdots$. It also is true that $\sin p\delta$ will have a maximum value less than unity for

$$\delta = r[\pi/(2q + 1)] \tag{57}$$

where $r = 1, 2, 3, 4, \cdots$.

The values of s/f corresponding to these values of δ and the resultant values of maximum $k_{10} \sin p\delta$ are given in Table I. Column 5 shows the ratio of k_{10} to the maximum of $k_{10} \sin p\delta$, and is a measure of the error

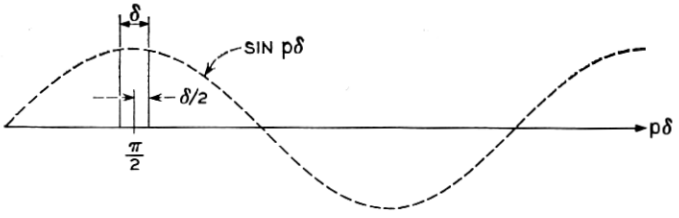

Fig. 13 — Diagram of $\sin p\delta$ yielding $|\sin p\delta| < 1$ for all p.

TABLE I

1 δ	2 s/f	3 k_{10}	4 Max. Value of $k_{10} \sin p\delta$	5 Column 3 ÷ Column 4
$\pi/2$	2	1.0	1.0	1.0
$\pi/3$	1	1.15	1.0	1.15
$2\pi/3$	3	1.15	1.0	1.15
$\pi/5$	0.38	1.70	1.62	1.05
$2\pi/5$	1.38	1.05	1.0	1.05
$3\pi/5$	2.62	1.05	1.0	1.05
$4\pi/5$	3.62	1.70	1.62	1.05
$\pi/7$	0.194	2.31	2.255	1.023
$2\pi/7$	0.750	1.28	1.25	1.023
$3\pi/7$	1.554	1.023	1.0	1.023
$4\pi/7$	2.444	1.023	1.0	1.023
$5\pi/7$	3.226	1.28	1.25	1.023
$6\pi/7$	3.806	2.31	2.255	1.023

made in assuming sin $p\delta$ goes through unity. That ratio is $1/\cos(\delta/2)$ where δ is given by (56). All values for a given q in (57) result in the same error, but the various values of r indicate the values of δ and s/f at which that error will appear. Fig. 14 summarizes the data of Table I; for p ranging up to infinity it is only at the discrete values of δ given by (57) that the maximum of $k_{10} \sin p\delta$ differs from k_{10}.

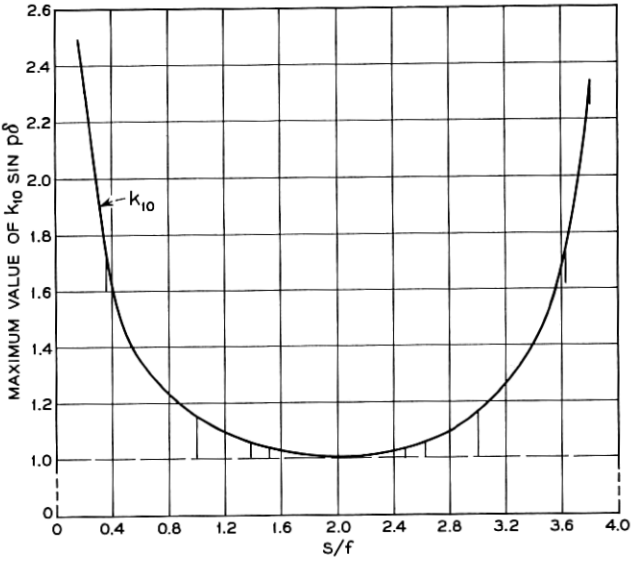

Fig. 14 — Maximum value of $k_{10} \sin p\delta$ vs s/f.

If p were finite and the ratio s/f was varied, the plot of Fig. 14 would presumably show finite-width dips of the same over-all depth as those plotted.

APPENDIX B

It is the purpose of this appendix to point out that the "thin lens" description of light ray propagation leads to the following conclusion (see Fig. 15):

The slope and displacement of the output ray of an arbitrary sequence of lenses for an input ray of slope r_0' and displacement r_1 is exactly the algebraic sum of the slopes and displacements of the output ray found (*i*) for an input ray of slope r_0' with zero displacement from the axis, and assuming all lens displacements $d_n = 0$, (*ii*) for an input ray of displacement r_1 with zero slope and assuming all lens displacements $d_n = 0$, and (*iii*) for an input ray of zero slope and zero displacement and assuming one lens displacement at a time is nonzero, summing the ray output slopes and displacements thus found over all lens displacements.

The proof is as follows: For the nth lens in a sequence of lenses (see Fig. 1):

$$r_n' = r_{n-1}' - \left(\frac{r_n - d_n}{f_n}\right) \tag{58}$$

where r_n' is the slope of the ray immediately following the nth lens and r_n is the displacement at the nth lens. We note that the angular lens rotation φ_n does not affect the ray propagation, an approximation which implies that

$$(r_n - d_n) \cos \varphi_n \cong (r_n - d_n) \tag{59}$$

or

$$\varphi_n \ll 1.$$

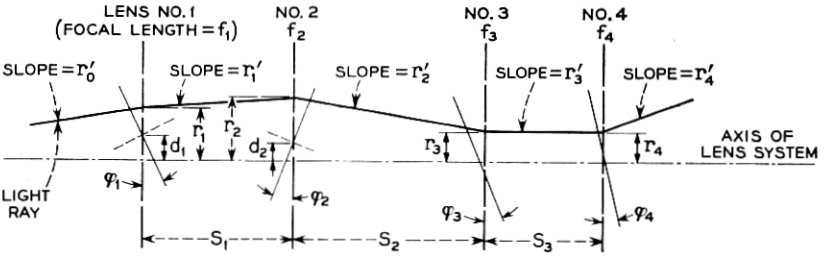

Fig. 15 — Light-ray path in an arbitrary lens system.

We may expand (58) to form

$$r_n' = r_0' - \frac{(r_1 - d_1)}{f_1} - \frac{(r_2 - d_2)}{f_2} \cdots - \frac{(r_n - d_n)}{f_n}. \tag{60}$$

Similarly, the displacement r_n at the nth lens is

$$r_n = r_{n-1} + s_{n-1} r_{n-1}' \tag{61}$$

which may be expanded to

$$r_n = r_{n-1} + s_{n-1} \left\{ r_0' - \frac{(r_1 - d_1)}{f_1} - \frac{(r_2 - d_2)}{f_2} \cdots - \frac{(r_{n-1} - d_{n-1})}{f_{n-1}} \right\} \tag{62}$$

which is valid for $n \geqq 2$.

We may examine each term of (60) and (62) and find that

$$r_n' = A_n r_0' + B_n r_1 + \sum_{m=1}^{m=n} \alpha_m \frac{d_m}{f_m} \tag{63}$$

$$r_n = C_n r_0' + D_n r_1 + \sum_{m=1}^{m=n} \beta_m \frac{d_m}{f_m} \tag{64}$$

in which A_n, B_n, C_n, D_n and the α_m and β_m are all independent of r_0', r_1 and the d_m.

We have thus proven the above-stated conclusion.

REFERENCES

1. Pierce, J. R., *Theory and Design of Electron Beams*, 2nd ed., D. Van Nostrand, Princeton, 1954.
2. Courant, E. D., Livingston, M. S., and Snyder, H. S., The Strong-Focusing Synchrotron — A New High-Energy Accelerator, Phys. Rev., **88**, Dec. 1, 1952, pp. 1190–1196.
3. Boyd, G. D., and Kogelnik, H., Generalized Confocal Resonator Theory, B.S.T.J., **41**, July, 1962, pp. 1347-1369.